Journal of Alloys and Compounds 503 (2010) 410–415

Contents lists available at ScienceDirect

Journal of Alloys and Compounds

journal homepage: www.elsevier.com/locate/jallcom

Microstructural characteristics of spray formed zircon sand reinforced LM13 composite

Kamalpreet Kaur, O.P. Pandey*

School of Physics & Materials Science, Thapar University, Patiala, Punjab 147 004, India

ARTICLE INFO

Article history:
Received 13 October 2009
Received in revised form 23 April 2010
Accepted 28 April 2010
Available online 11 May 2010

Keywords:
Aluminium metal matrix composite
Rapid solidification
Scanning electron microscope (SEM)

ABSTRACT

Aluminum metal matrix composites (MMC) are one of the attractive light weight substance which find their application in automotive and aerospace industries. In the present work spray forming technique has been used to prepare zircon sand reinforced LM13 alloy. The spray formed composite and base alloy were characterized using optical and scanning electron microscopes. The thermal analysis of the base alloy, zircon sand particles and reinforced composite has been done with differential thermal analyzer and dilatometer to see its applicability at high temperature. The microstructural features and hardness of spray formed LM13/zircon sand composite revealed equiaxed morphology with nearly uniform distribution of zircon sand particles in the middle of preform as well as good particle/matrix interfacial bonding. The linear expansion coefficient of base alloy is found to be $8.67 \times 10^{-6}\,K^{-1}$ and for spray formed composite is $8.38 \times 10^{-6}\,K^{-1}$ (5% V_f of zircon sand) and $9.11 \times 10^{-6}\,K^{-1}$ (15% V_f of zircon sand) in 25–465 °C temperature limit, which is quite comparable indicating good interfacial bonding.

1. Introduction

The requirement of fuel efficiency and pollution control in transport system has led to development of high performance light weight alloys. Al–Si alloys are one of the deserving candidates for this class due to their low coefficient of thermal expansion, good machinability and greater strength to weight ratio. Enhancement in performance can be attained with microstructural homogeneity of second phase. Conventionally die-casting and powder metallurgical process are used for manufacturing of Al/Al-alloy composites at large scale. A novel technique of extending solid solubility was developed in 1960 by Duwez et al. [1] with Ag–Cu alloys achieving high rates of cooling. Also, metastable solid solution has been generated by cooling rapidly enough to forestall the normal nucleation and growth processes in ternary system [2]. Further Singer [3] gave near net-shape spray processing technique under rapid solidification processes. Now a day the spray forming process has been adopted as a new route to solve the problems of macrosegregation, agglomeration of reinforced particles, increasing the solid solubility range with achieving cost effective near net-shape systems with superior mechanical properties [4,5].

In the rapid solidification process of spray forming high velocity inert gas jets disintegrate the stream of molten metal/alloy into micron-sized droplets, called atomization. Further under the effect of gravity and gas jets, the atomized droplets are propelled down and collected on the conductive substrate giving rise to the formation of highly dense preform called deposit. Over past three decades efforts are being made to utilize this technique for the preparation of particle reinforced metal matrix composites (MMCs). The advantages of spray forming have stimulated interest in industries towards its technological potential to use it commercially. Many researchers worked on different combination of Al-based alloys and intermetallic compounds [5]. Moreover, the reinforcing particles which are commonly used are Al_2O_3 [6], SiC [7–9], graphite [9], TiB_2 [10], TiC [11] and transition elements like Ni and Ce [12]. Limited work has been done on zircon sand reinforced Al-alloy composite. A comparative wear study of stir cast zircon sand and alumina reinforced Al–4.5% Cu alloy has been investigated by Das et al. [13] and found that zircon sand particulates offer greater resistance to abrasive wear as compared to the alumina reinforcement. The age hardening study of same composite shows that the microhardness of age hardenable Al–Cu based alloy composites depend on the quenching medium [14].

Till now spray forming process has not been utilized to form zircon sand reinforcement in the Al–Si matrix. In the present work commercially used piston alloy (LM13 alloy) containing approximately 1% Mg has been chosen for the work. The wettability of the particles in the Al-base matrix can be enhanced by Mg since it scarves the gases and oxygen from the particulate surface making it more reactive [15,16]. Further, the thermal stability and linear coefficient of thermal expansion of the both alloy and reinforced

* Corresponding author. Tel.: +91 175 2393116; fax: +91 175 2393005.
E-mail address: oppandey@thapar.edu (O.P. Pandey).

0925-8388/$ – see front matter © 2010 Elsevier B.V. All rights reserved.
doi:10.1016/j.jallcom.2010.04.249

Table 1
Composition of the alloy in wt.%.

LM13 alloy	Si	Fe	Cu	Mn	Mg	Zn	Ti	Ni	Pb	Sn	Al
XRF	11.166	0.332	1.247	0.598	0.849	0.250	0.026	0.868	0.001	0.002	Balance
Wet chemical analysis	11.800	0.365	1.230	0.411	0.940	0.210	0.0254	0.940	0.0289	0.005	Balance

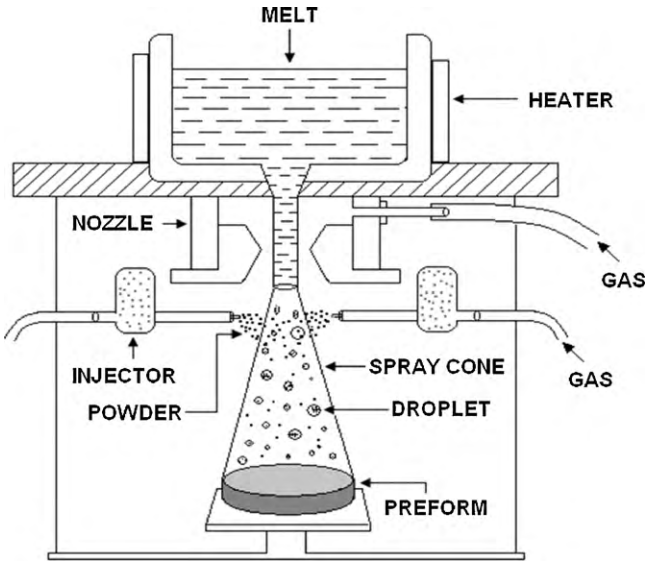

Fig. 1. Schematic diagram of spray forming process.

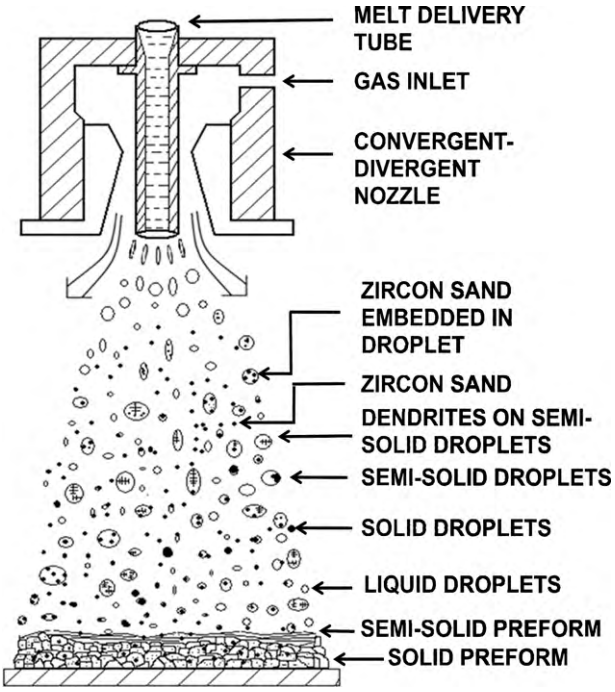

Fig. 2. Schematic diagram of convergent–divergent nozzle with preform deposition.

composite has been analyzed to see the feasibility of its application in the automotive industry.

2. Experimental procedures

LM13 alloy was obtained in the form of ingots. The compositional analysis of the alloy was done by wet chemical analysis. This composition was further confirmed by X-ray florescence technique which is shown in Table 1. The aluminum matrix composite (AMC) material has been prepared by spray forming process. The schematic diagram of the spray forming process is shown in Fig. 1.

The indigenously designed and fabricated convergent–divergent atomizer (Fig. 2) is used for gas atomization and spray deposition. For spray deposition, 1.5 kg charge of LM13 alloy was melted at 800 °C in a graphite crucible under nitrogen atmosphere in a resistance furnace. On reaching the desirable temperature, the alloy was poured into a preheated crucible attached above the atomizer assembly. Before pouring the molten alloy high pressure (0.7 MPa) nitrogen gas was passed through the atomizer. The melt flows through the melt delivery tube of inner diameter of 8 mm concentrically fixed in the convergent–divergent atomizer. Simultaneously, preheated zircon sand particles (sieved in the particle range size 106–125 μm) are fed into the spray cone with the help of two external powder injectors having orifice of 1 mm placed around the melt atomizing section. The nozzle to substrate distance was kept at 300 mm. The atomized droplets get collected on the stationary copper substrate to make a solid preform of diameter 150 mm and thickness of 30 mm as shown in Fig. 2. From the preform, samples of dimensions 25 mm × 15 mm × 15 mm were cut from different areas of the preform for further characterization. The LM13 alloy and spray formed composites were mechanically polished and etched with Keller's reagent before microstructural analysis.

The microstructural analysis has been done with the help of both optical (Eclipse MA-100, Nikon) and scanning electron microscope (JEOL, Japan) at various magnifications. The bulk hardness of the LM13/Zircon sand composite and LM13 alloy has been measured by Brinell hardness tester using 5 mm diameter steel ball indenter under 250 kgf load. The average value of five indentations per sample has been taken. Microhardness of the different phases was measured using microhardness tester (Micromet II B-M83174, Buehler USA). Microhardness measurement was done on each set of sample by taking minimum of five indentations per sample at 0.05 kgf load.

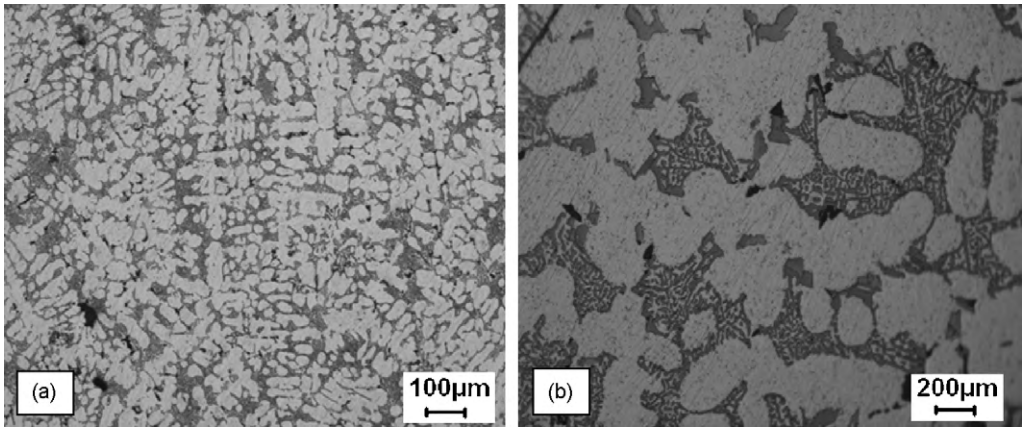

Fig. 3. Optical micrographs of as cast LM13 alloy at (a) low and (b) high magnification showing dendritic morphology.

Table 2
Variation in microhardness of LM13/zircon sand composite at different areas.

On the particle (H_V)	At the interface (H_V)	On the matrix (H_V)
904	113	80

The thermal kinetics of the composite was studied using differential thermal analysis (Perkin Elmer Diamond TG/DTA) to check the phase transition with variation in temperature. The samples were heated in nitrogen atmosphere placed in platinum crucible taking alumina as reference material with a heating rate of 5 °C/min in the range of 50–570 °C. The thermal expansion coefficient (TEC) of the base alloy and prepared composite was measured using Netzch DIL 402 PC dilatometer in the temperature range 29–470 °C of 25 mm long samples. All thermal measurements were done to check its suitability for high temperature applications.

3. Results and discussion

Bulk hardness and microhardness measurement of both reinforced and unreinforced specimens was done to know the effect of reinforced particulates on the base LM13 alloy hardness. The results show that zircon sand particulates increase the bulk hardness of the base LM13 alloy from 76.3 BHN to 83.7 BHN. Moreover, in spray processing route microstructural refinement of the composite by rapid solidification lead to increase in the hardness value. Microhardness indentations have been carried out on the embedded zircon sand particles as well as in the vicinity of particles. The average microhardness values are given in Table 2. A trend of microhardness is observed to decrease as we move far from the particle. However, the overall hardness of the material has increased as indicated by bulk hardness measurement. This also confirmed the good interfacial bonding between the particles and the matrix.

The optical micrograph of the as cast LM13 alloy (Fig. 3a) shows the dendritic growth of α-Al grains and eutectic phase in between the interdendritic arms (Fig. 3b). Fig. 4(a and b) shows the microstructure of spray formed alloy with the reinforcement of zircon sand particulates in the LM13 matrix. The zircon sand particles can be seen as well embedded in the matrix as shown in Fig. 4(c and d) with no closed porosity at the interfacial zone of particle and matrix. The equiaxed α-Al grains of 25–50 μm size are observed in the LM13/zircon sand composite. The equiaxed microstructural features have been reported widely in spray forming by other researchers [17]. This equiaxed morphology can be explained on the basis of shearing effect produced in spray atomization. The high velocity oncoming gas first interacts with molten metal stream. The molten metal stream gets sheared due to its interaction and comes out in the form of ligaments. This ligament is further broken into number of droplets due to its further interaction with gas in the atomizing zone causing shearing. Due to fast extraction of heat through the gas-droplet interface a high amount of kinetic undercooling is observed in the droplet. During the flight as solidification proceeds, nucleation occurs along the preferred sites forming the dendritic arms on the surface of spray droplets as shown in Fig. 2.

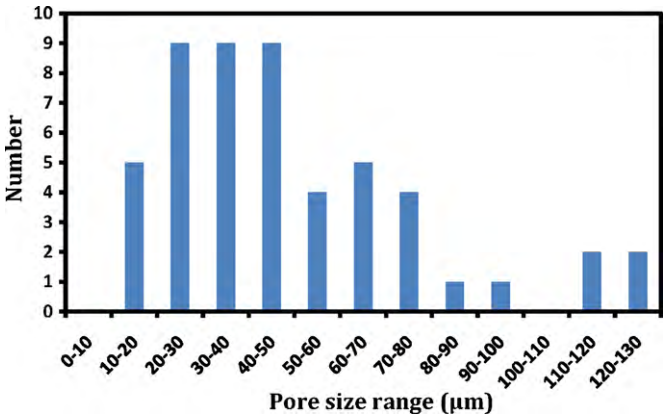

Fig. 5. Distribution of pores in the spray formed composite.

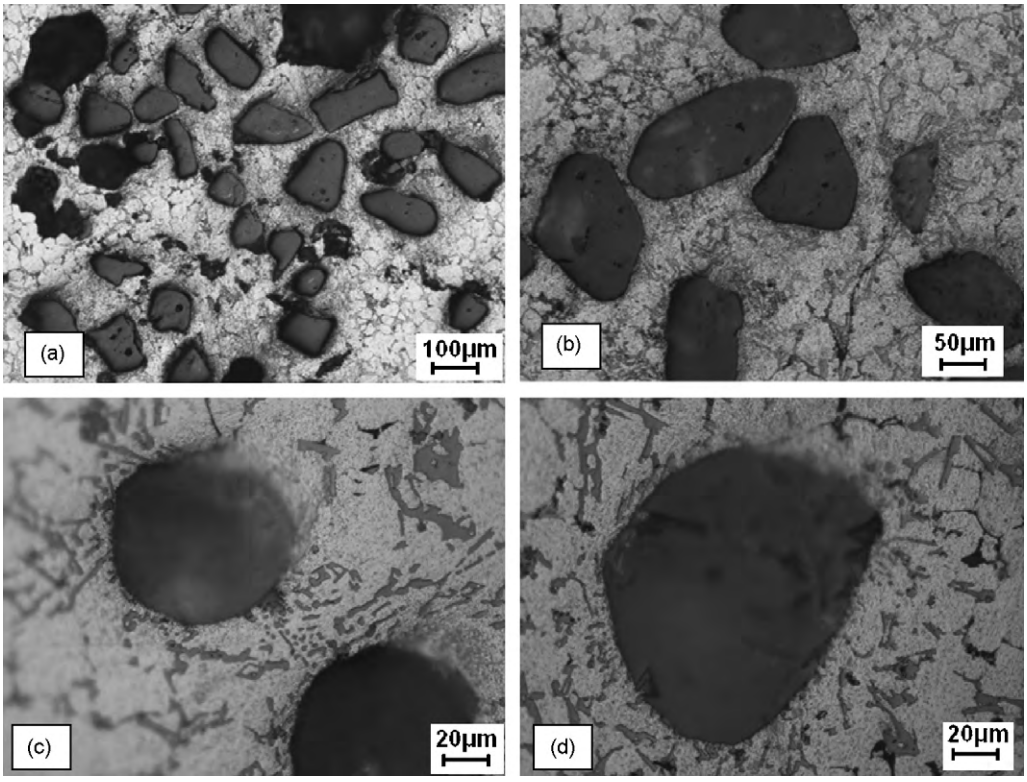

Fig. 4. Optical micrographs of spray formed LM13/zircon sand composite showing distribution of zircon sand particles (a and b) and interface morphology (c and d).

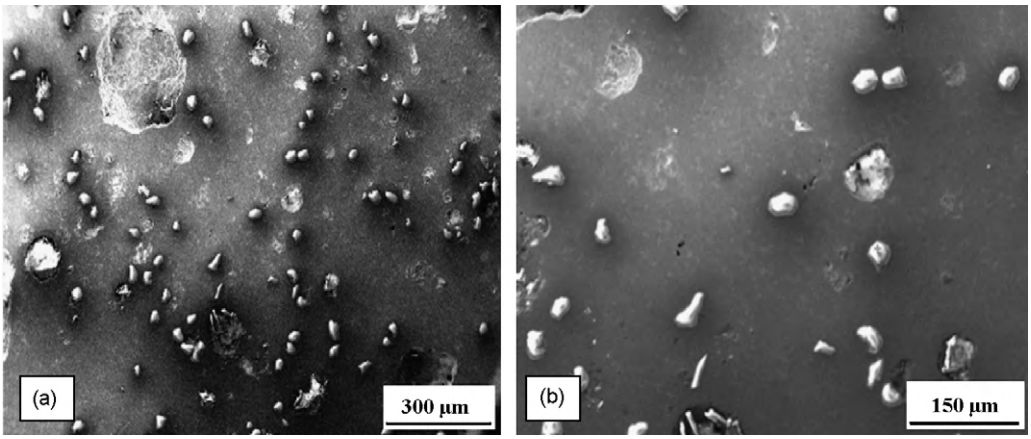

Fig. 6. SEM micrographs of spray formed LM13/zircon sand composite showing embedded particles of zircon sand (a and b).

The high velocity nitrogen gas jets produce perturbation on surface of these semi-solid droplets which in turn lead to further fragmentation of droplets and breakage of the dendritic arms on striking surface. On the mushy preform these broken dendritic arms float on the surface resulting in equiaxed grain morphology of spray formed composite [17]. The subsequent impingement of the droplets causes turbulent fluid flow and remelting of the deposited droplets [18]. The turbulent flow on the preform surface during deposition of droplets entraps air causing porosity in the resulted composite. The size of pores and their fraction in the deposit varies from top to bottom. It has been observed that in middle layer of the deposit the amount of porosity is less as compared to top and bottom layer. The variation of porosity from the top, middle and bottom part is 5.17%, 2.45% and 4.01% respectively. Moreover, both closed and interconnected pores are present in the preform. The closed pore-size varies between 15.16 μm and 128.64 μm. The distribution of pore-size has been shown in Fig. 5.

The structural features indicate a good interfacial bonding of zircon sand with matrix. Zircon sand particles provide nucleation site for solidification of Si also. As is evident from Fig. 4(c and d) that nearly 3–10 μm sized globular Si particles are present all along the vicinity of the embedded zircon sand particle. As we proceed away from the interface of zircon sand particles the Si needles were observed to be elongated. The size variation of nearly 15–25 μm in the form of long thin Si needles in the matrix was observed. The localized cooling effect produced by zircon sand particle around its vicinity led to such type of morphological changes. A large amount of thermal gradient exists between zircon sand particle (preheated up to 60 °C) and atomized droplets when zircon sand collides with the melt (heated up to 800 °C) in the atomization zone near the melt delivery tube. The particles get embedded in the molten alloy and extract heat at higher rates from the surrounding melt which give rise to localized rapid cooling effect during solidification. Because of this phenomenon the formation of small globular Si morphology in vicinity of zircon sand particle is observed. The cooling rate away from the interface slows down and because of this effect the silicon morphology changes from globular to needle shape. There are two types of heat transfer phenomenon which occurs during atomization. First due to the convection cooling by the atomizing gas and second by conduction cooling by ceramic particles. Apart from this the conductive surface of substrate and preform also participate in heat extraction leading to non-equilibrium solidification.

Das et al. [13] have developed zircon particles reinforced Al–4.5% Cu composite by stir casting technique. There is a difference in microstructural features obtained in both spray and stir processing techniques. The microstructural features of stir cast zircon reinforced composite indicate the smooth particle-matrix interface showing reaction phase around the particle. However, in spray formed composite such interfacial layering is not observed. In rapid solidification the Si particles do not get much time to diffuse and grow around the interfacial zone. Instead a morphological change in Si particle of globular shape has been observed near the particles. This variation in microstructure leads to variation in microhardness as shown in Table 2. The presence of good interfacial bonding and micron-sized globular Si around the zircon sand particle gives rise to higher microhardness at the interface as compared to the matrix (where the size of Si needles are bigger).

SEM micrographs taken at different magnifications (Fig. 6) showed the 15% V_f of distributed reinforced particles in the spray formed alloy in the middle of preform. However, at the periphery of the preform the particle V_f decreases to 5%. Hence, it is evident in both optical and SEM studies that the particles are well embedded in the matrix with good interfacial bonding showing no porosity at the interface of zircon sand particle and the matrix. This is further confirmed by energy dispersive spectroscopy (EDS) analysis along the interface and on the particle as shown in Fig. 7 and Fig. 8 respectively. The presence of all the four major elements (Al, Si, Zr, O) at the interface confirmed good bonding between particle and matrix phase. However, EDS on the zircon sand particle (Fig. 8) also confirmed the presence of Zr, O and Si elements as major constituents. However, the intensity of Al peak is less in this case as Al is absent in the zircon sand particle.

DTA plot as shown in Fig. 9 depicts that phase transformation is occurring in the LM13 alloy as well as composite. Fig. 9(i) and (ii) shows the transformation within the complete range of

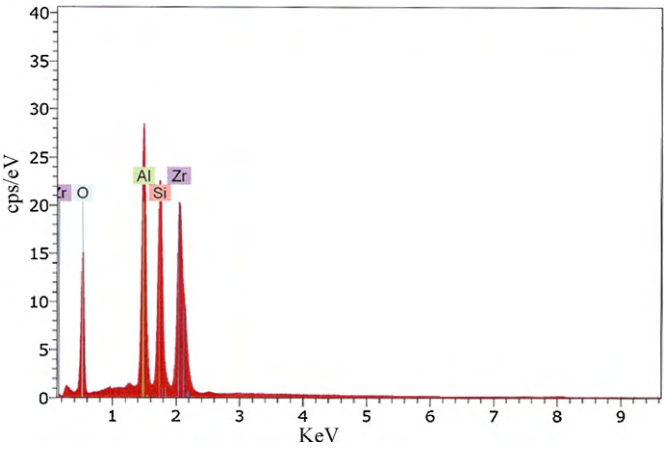

Fig. 7. EDS analysis of the sample at the interface of particle and matrix.

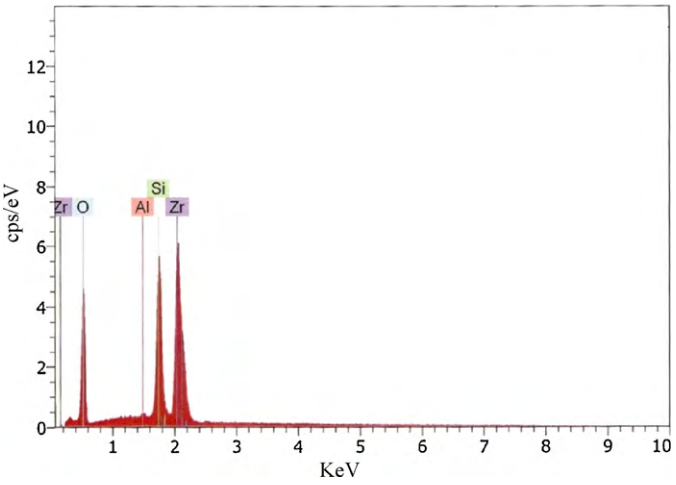

Fig. 8. EDS analysis of the sample on the zircon sand particle.

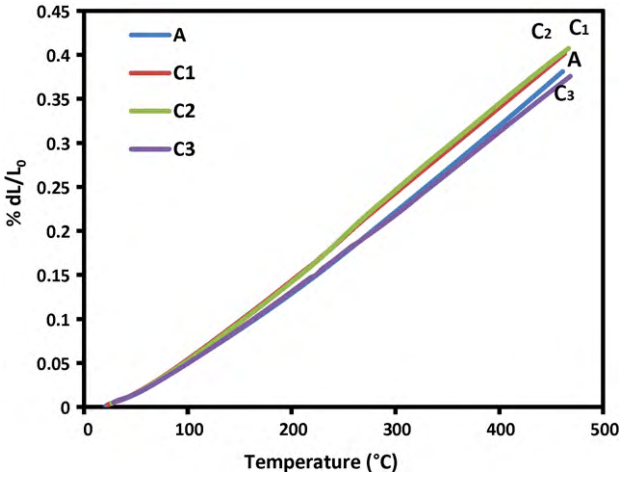

Fig. 10. Dilatometer plot of LM13 alloy (A), spray formed LM13/zircon sand composite (C); where C_1 and C_2 are for 15% V_f and C_3 for 5% V_f of zircon sand.

50–570 °C and enlarged view within 500–570 °C range respectively. First transformation is observed at 533 °C in case of both LM13 alloy and composite. This is because of softening effect when melting starts near liquidus line. The next alteration corresponds to the plateau in LM13 alloy at 542 °C, representing eutectic Al–Si transformation. However, in Al–Si system binary eutectic occur for 12.6 wt% Si at 577 °C. It has been found that the eutectic temperature get affected by the addition of Mg. Even a small amount of 0.1% Mg depresses the eutectic temperature by 10 °C [19]. In LM13 base alloy, the concentration of Mg is found to be approximately 0.9%. This leads to decrease Al–Si eutectic temperature by 35 °C. However, presence of other alloying elements in the alloy also affects the eutectic temperature. At this temperature, LM13/zircon sand reinforced composite exhibits a steep change instead of plateau. This might be due to the stress relaxation at the interfacial zone of zircon sand and matrix. There is no such exothermic peak observed in zircon sand which shows absence of phase transition in zircon sand for the reason that the melting temperature of the zircon sand is quite high. The change in slope at 552 °C temperature and the plateau corresponds to the next eutectic transformation of ternary system (Al–Si–Mg). However, this transformation is due to intermetallic compound magnesium silicide (Mg_2Si) which shows non variant phase reaction at 555 °C [20] as given in Eq. (1) below:

$$L \rightarrow Al + Si + Mg_2Si \quad (1)$$

Similarly, linear thermal expansion of LM13 alloy (A) and the sprayed formed composite (C) is calculated by dilatometery test which is given in Fig. 10. The thermal expansion coefficient (TEC) of alloy and sprayed composite are measured as a function of temperature which is shown in Fig. 11. TEC measurements were performed to see the feasibility of replacement of LM13 alloy with

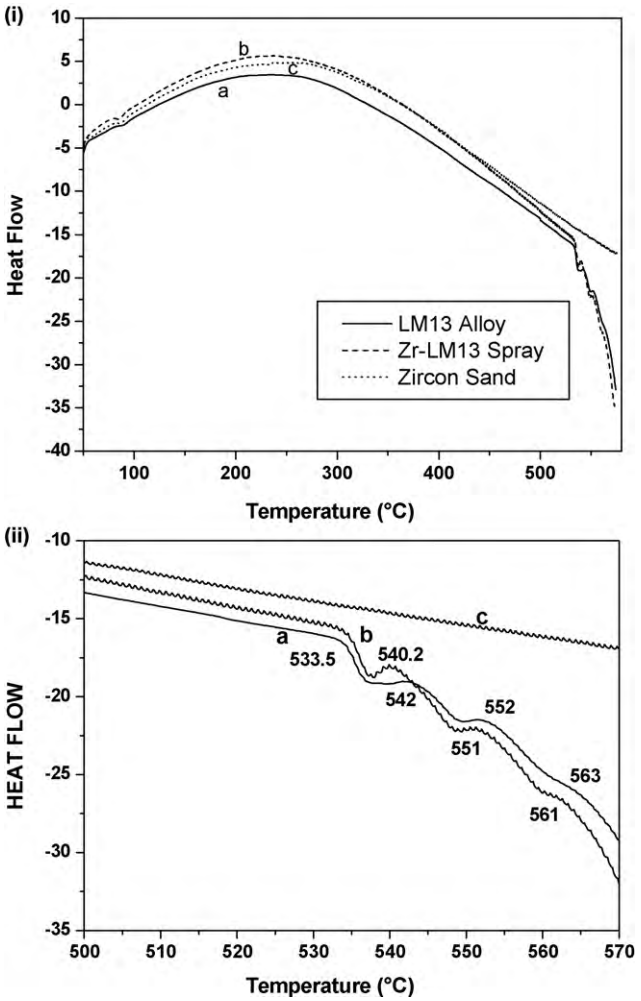

Fig. 9. DTA plot of (a) cast LM13 alloy (b) spray deposited LM13/zircon sand and (c) zircon sand (i) from 50 to 570 °C and (ii) from 500 to 570 °C.

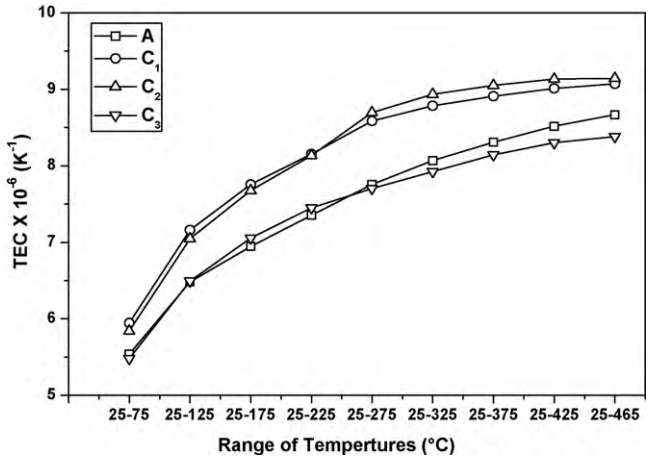

Fig. 11. Measured value of TEC in different temperature ranges for LM13 alloy (A) and spray formed LM13/zircon sand composite (C); C_1, C_2 (V_f = 15%) and C_3 (V_f = 5%).

LM13/zircon sand composite. The percentage variation in change in length showed a linear trend with respect to the temperature (Fig. 10). Fig. 11 showed that the values of TEC are similar for A and C_3 (V_f = 5%). However, following the similar trend C_1 and C_2 (V_f = 15%) showed a little increase in the TEC. The TEC variation corresponds to the distribution of zircon sand particles in the composite. The particulate volume fraction is found to be greater in the middle of the preform as compare to the periphery region. In 25–75 °C temperature range TEC of LM13 alloy is found to be 6.5% lower than 15% V_f zircon sand reinforced specimen. Moreover, this value corresponds to an increase of 1% from the specimen taken from 5% V_f zircon sand reinforced specimen. Within higher temperature range 25–465 °C an increase of 5% have been noticed for C_1 and C_2 as compared to A. However, a 3.3% decrease of TEC value for C_3 to that of unreinforced sample has been observed. The variation for C_3 might be due to the presence of porosity in spray deposited preform.

The interfacial bonding of zircon sand with aluminium matrix is strong. Presence of pores in the spray formed sample may lead to deviation from its linear to zigzag character at high temperature. In our DTA measurement the linear character of zircon sand is observed which indicate that no phase transformation is taking place. It is also expected that zircon sand may not lead to deviation in dilatometer test which has been already demonstrated (Fig. 10). At higher temperature slight deviation may occur because of porosity due to entrapped gases during atomization. The above test confirms that the composite processed by spray forming technique can provide a better substitute having superior strength to the conventionally used LM13 alloy.

4. Conclusions

The zircon sand reinforced Al–Si alloy composite has been successfully prepared using spray deposition technique. Zircon sand particles show good bonding in the matrix as revealed from the optical and SEM study which is further confirmed by microhardness measurement. Also the bulk hardness is found to increase with addition of zircon sand particles in LM13 alloy. Wide difference in the morphology is observed for as cast alloy and spray processed composite. Despite of dendritic growth of α-Al grains in ingot casted alloy, equiaxed grains of α-Al are obtained in spray formed composite. Moreover, 3–10 μm sized globular Si particles along the interface and 15–25 μm sized Si particles in the matrix are observed in spray processed LM13/zircon sand composite indicating an induced rapid solidification effect. The DTA plots illustrate the pseudo-binary eutectic reaction as well as the depression in the Al–Si eutectic reactions in the base alloy and composite. There is a small variation in the TEC values for spray formed composite sample for 5% and 15% V_f of zircon sand. However, the spray formed composite is thermally stable as confirmed by TEC which is comparable to the base alloy.

Acknowledgment

The authors would like to acknowledge the financial support of Council of Scientific & Industrial Research (CSIR), Scheme No. 22(0403)/06/EMR-II, Government of India for carrying out the research work.

References

[1] P. Duwez, R.H. Willens, W. Klement Jr., Journal of Applied Physics 31 (1960) 1136–1137.
[2] P. Duwez, R.H. Willens, W. Klement Jr., Journal of Applied Physics 31 (1960) 1500.
[3] A.R.E. Singer, Metals and Materials 4 (1970) 246–250.
[4] W.J. Kim, J.H. Yeon, J.C. Lee, Journal of Alloys and Compounds 308 (1–2) (2000) 237–243.
[5] L.A. Beret, C.F. Ferrarini, W.J. Botta F., C.S. Kiminami, C. Bolfarini, Journal of Alloys and Compounds 434–435 (2007) 371–375.
[6] M. Anil, S. Ojha, Journal of Materials Science 41 (4) (2006) 1073–1080.
[7] C. Zhenhua, T. Jie, C. Gang, F. Dingfa, Y. Hongge, Wear 262 (2007) 362–368.
[8] E.G. Gomes, J.L. Rossi, Materials Science Forum 498–499 (2005) 251–256.
[9] J. Zhang, R.J. Perez, E.J. Lavernia, Acta Metallurgica et Materialia 42 (2) (1994) 395–409.
[10] M.A. Herbert, R. Maiti, R. Mitra, M. Chakraborty, Wear 265 (2008) 1606–1618.
[11] B. Yang, F. Wang, J.S. Zhang, Acta Materialia 57 (17) (2003) 4977–4989.
[12] T.H. Lee, S.J. Hong, Journal of Alloys and Compounds 487 (2009) 218–224.
[13] S. Das, S. Das, K. Das, Composite Science and Technology 67 (2007) 746–751.
[14] A. Sharma, S. Das, Materials and Design 30 (2009) 3900–3903.
[15] B.C. Pai, G. Ramani, R.M. Pillai, K.G. Satyanarayana, Journal of Materials Science 30 (1995) 1903–1911.
[16] A. Banerji, M.K. Surappa, P.K. Rohatgi, Metallurgical and Materials Transactions B 14 (2) (1983) 273–283.
[17] V.C. Srivastava, R.K. Mandal, S.N. Ojha, Materials Science and Engineering A 304–306 (2001) 555–558.
[18] S.K. Chaudhury, S.C. Panigrahi, Journal of Materials Processing Technology 182 (1–3) (2007) 343–351.
[19] Handbook of Aluminum, in: G.E. Totten, D.S. Mackenzie (Eds), Physical metallurgy and processes, vol.1, CRC press, 2003, ISBN 0824704940.
[20] Casting aluminium alloys, in: V.S. Zolotorevskiĭ, N.A. Belov, M.V. Glazoff, (Eds), Elsevier, 2007, ISBN 0080453708.